

Spin-orbital entanglement near quantum phase transitions

Andrzej M. Oleś^{*1,2}, Peter Horsch¹, and Giniyat Khaliullin^{1,3}

¹ Max-Planck-Institut für Festkörperforschung, Heisenbergstrasse 1, D-70569 Stuttgart, Germany

² M. Smoluchowski Institute of Physics, Jagellonian University, Reymonta 4, PL-30059 Kraków, Poland

³ Kazan Physical-Technical Institute of the Russian Academy of Sciences, 420029 Kazan, Russia

Received 29 September 2006, accepted 3 December 2006

PACS 75.10.Jm, 03.67.Mn, 71.70.Ej, 73.43.Nq

Spin-orbital entanglement in the ground state of a one-dimensional $SU(2) \otimes SU(2)$ spin-orbital model is analyzed using exact diagonalization of finite chains. For $S = 1/2$ spins and $T = 1/2$ pseudospins one finds that the quantum entanglement is similar at the $SU(4)$ symmetry point and in the spin-orbital valence bond state. We also show that quantum transitions in spin-orbital models turn out to be continuous under certain circumstances, in contrast to the discontinuous transitions in spin models with $SU(2)$ symmetry. [Published in: *Phys. Status Solidi (b)* **244**, 2378-2383 (2007).]

Copyright line will be provided by the publisher

Rich magnetic phase diagrams of transition metal oxides and the existence of quite complex magnetic order with coexisting ferromagnetic (FM) and antiferromagnetic (AF) interactions, such as A -AF phase in LaMnO_3 or C -AF phase in LaVO_3 , originate from the intricate interplay between spin and orbital degrees of freedom — alternating orbital (AO) order supports FM interactions, whereas ferro orbital (FO) order supports AF ones [1]. While in many cases the spin and orbital dynamics are independent from each other and such classical concepts apply, the quantum fluctuations are *a priori* enhanced due to a potential possibility of joint *spin-orbital* fluctuations, particularly in the vicinity of quantum phase transitions [2]. Such fluctuations are even much stronger in t_{2g} than in e_g systems and may dominate the magnetic and orbital correlations [3], which could then contradict the above classical expectations in certain regimes of parameters. Recently it has been realized [4] that this novel quantum behavior is accompanied by spin-orbital entanglement, similar to that being currently under investigation in spin models [5].

In general, any spin-orbital superexchange model derived for a transition metal compound with a perovskite lattice may be written in the following form:

$$\mathcal{H} = J \sum_{\gamma} \sum_{\langle ij \rangle \parallel \gamma} \left[\left(\vec{S}_i \cdot \vec{S}_j + S^2 \right) \hat{J}_{ij}^{(\gamma)} + \hat{K}_{ij}^{(\gamma)} \right] + \mathcal{H}_{\text{orb}}, \quad (1)$$

where $\gamma = a, b, c$ labels the cubic axes — depending on the direction of a bond $\langle ij \rangle$ the interactions take a different form. The first term in Eq. (1) describes the superexchange interactions ($J = 4t^2/U$ is the superexchange constant, where t is the hopping element and U stands for the Coulomb element) between transition metal ions in the d^n configuration with spin S . The orbital operators $\hat{J}_{ij}^{(\gamma)}$ and $\hat{K}_{ij}^{(\gamma)}$ depend on Hund's exchange parameter $\eta = J_H/U$, which determines the excitation spectra after a virtual $d_i^n d_j^n \rightarrow d_i^{n+1} d_j^{n-1}$ charge excitation. Therefore, realistic models of this type (some examples were given recently in Ref. [6] and analyzed using the mean field approximation in Ref. [7]) are rather involved and contain several terms). In addition, orbital interactions can also be induced by the coupling to the lattice, and appear in \mathcal{H}_{orb} term which depends on a second parameter V .

In the limit of $\eta = 0$, however, and for t_{2g} orbitals, $\hat{J}_{ij}^{(\gamma)}$ and $\hat{K}_{ij}^{(\gamma)}$ operators simplify and contain only a scalar product $\vec{T}_i \cdot \vec{T}_j$ of $T = 1/2$ pseudospin operators which stand for two active t_{2g} orbitals along

* Corresponding author: e-mail: a.m.oles@fkf.mpg.de

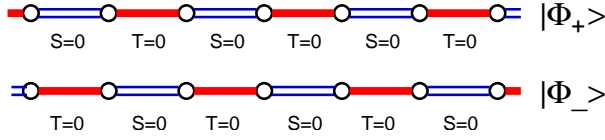


Fig. 1 Two degenerate SOVB ground states $|\Phi_{\pm}\rangle$ with alternating spin ($S = 0$) and orbital ($T = 0$) singlets for the $SU(2)\times SU(2)$ model (5) at the dimer point $p = 3/4$.

γ , so the $SU(2)$ symmetry follows both for spin and for pseudospin interactions. Here we shall discuss primarily a one-dimensional (1D) model in this idealized situation and investigate the dependence of spin-orbital entanglement on the type of underlying interactions. To characterize the ground state we evaluated intersite spin, orbital and composite spin-orbital correlations, defined as follows for a bond $\langle ij \rangle$ [4]:

$$S_{ij} = \langle \vec{S}_i \cdot \vec{S}_j \rangle / (2S)^2, \quad T_{ij} = \langle \vec{T}_i \cdot \vec{T}_j \rangle, \quad (2)$$

$$C_{ij} = [\langle (\vec{S}_i \cdot \vec{S}_j)(\vec{T}_i \cdot \vec{T}_j) \rangle - \langle \vec{S}_i \cdot \vec{S}_j \rangle \langle \vec{T}_i \cdot \vec{T}_j \rangle] / (2S)^2. \quad (3)$$

Note that C_{ij} quantifies the quantum entanglement — if $C_{ij} < 0$ spin and orbital operators are entangled and mean field approximation, i.e., decoupling of spin and pseudospin operators is not justified.

The 1D $SU(2)\times SU(2)$ model,

$$\mathcal{H}_J = J \sum_i \left(\vec{S}_i \cdot \vec{S}_{i+1} + x \right) \left(\vec{T}_i \cdot \vec{T}_{i+1} + y \right), \quad (4)$$

has two parameters x and y . Its phase diagram in the (x, y) plane consists of five distinct phases which result from the competition between effective AF and FM spin (AO and FO pseudospin) interactions on the bonds [8]. First of all, the spin and pseudospin correlations are FM-FO, $S_{ij} = T_{ij} = \frac{1}{4}$, if $x < -\frac{1}{4}$ and $y < -\frac{1}{4}$. Then the ground state is characterized by the maximal values of both total quantum numbers, $S = T = N/2$, where N is the chain length, its degeneracy is $d = (N+1)^2$, and the quantum fluctuations are suppressed. Two other phases, with either spin FM or pseudospin FO correlations, show also no entanglement as the wave function factorizes, i.e., spin and orbital operators may be then still decoupled from each other. In these cases only either spin or pseudospin quantum fluctuations occur. On the contrary, in the other two phases both spin and orbital correlations are negative [9], so one expects that quantum entanglement takes over.

This motivates our study of the $SU(2)\otimes SU(2)$ model along the line $p = x = y$, where $S = 1/2$ spins and $T = 1/2$ pseudospins appear on equal footing. However, in order to allow also for a larger value of spin S per site, we write the Hamiltonian along this line in the following way,

$$\mathcal{H}_J = J \sum_i \left(\vec{S}_i \cdot \vec{S}_{i+1} + \frac{4}{3}pS(S+1) \right) \left(\vec{T}_i \cdot \vec{T}_{i+1} + p \right), \quad (5)$$

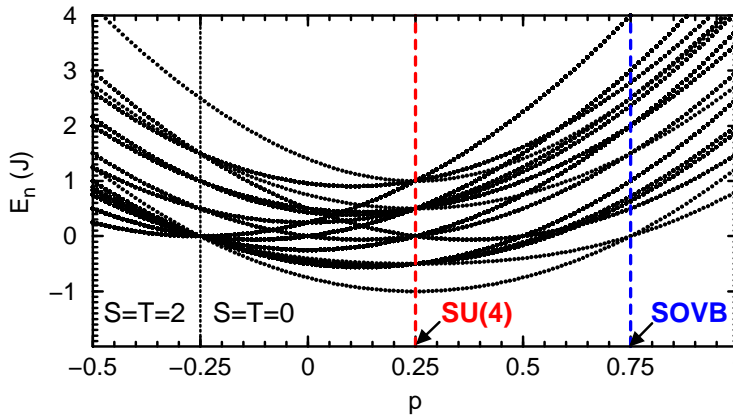


Fig. 2 Energy spectrum for the $S = 1/2$ spin-orbital chain (5) of $N = 4$ sites for increasing p . Some of the 256 eigenenergies have high degeneracy d . At $p = -0.25$ the ground state changes from high spin-orbital state ($S = T = 2$, $d = 25$) to spin-orbital singlet state ($S = T = 0$, $d = 1$); its degeneracy at $p = -0.25$ is $d = 194$. The $SU(4)$ point ($p = 0.25$, $d = 1$) and the SOVB point ($p = 0.75$, $d = 2$) are marked by vertical dashed lines.

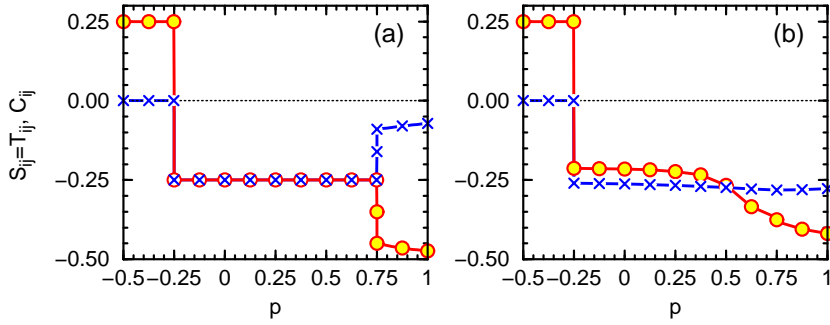


Fig. 3 Intersite spin and orbital correlations $S_{ij} = T_{ij}$ (2) (circles), and composite spin-orbital correlations C_{ij} (3) (crosses), as obtained for the 1D spin-orbital chains for increasing p in Eq. (5), with: (a) $N = 4$, and (b) $N = 8$ sites.

with $\frac{4}{3}pS(S+1) = p$ for $S = 1/2$. Interestingly, for $p = \frac{3}{4}$ the model given by Eq. (5) has an exact doubly degenerate ground state $|\Phi_{\pm}\rangle$, with alternating spin and orbital singlets forming a spin-orbital valence bond (SOVB) phase (Fig. 1). These states resemble the Majumdar-Ghosh valence bond states in the 1D spin model with next-nearest interactions [10] and have exact energy $E_0 = 0$ given by either spin or orbital singlet. Each $|\Phi_{\pm}\rangle$ state is a matrix product state in both spin and orbital sector [11]. For $S = 1/2$ and $p = \frac{1}{4}$ one recovers the celebrated SU(4) model, with all three correlation functions: S_{ij} , T_{ij} , and $\frac{4}{3}\langle(\vec{S}_i \cdot \vec{S}_{i+1})(\vec{T}_i \cdot \vec{T}_{i+1})\rangle$ being equal to each other [12]. The energy spectra in these two cases look quite differently for an $N = 4$ site chain — an equidistant energy spectrum with high degeneracies of each excited state with energies $(-1 + \frac{n}{2})J$ where $n = 0, 1, \dots, 4$ is found at the SU(4) point, while the spectrum consists of many eigenenergies with lower degeneracies at the SOVB point (Fig. 2). It is *a priori* not clear in which of these two points the quantum entanglement is stronger, but one might expect that it would be more pronounced at the SU(4) point.

In fact, it was shown recently that a reduced von Neumann entropy is there maximal [13]. While the spin-orbital entropy could help to understand the consequences of the entanglement at finite temperature which might trigger phase transitions to phases with strong dimer correlations [14] observed in experiment [15], here we suggest that a useful measure of *entanglement in the ground state* is the intersite spin-orbital correlation function (3) which quantifies the error of the mean field decoupling of spin and orbital operators on individual bonds. The intersite spin, orbital and spin-orbital correlations demonstrate a quantum phase transition between the high spin-orbital FM-FO state ($S = \mathcal{T} = 2$) and the singlet entangled state ($S = \mathcal{T} = 0$) at $p = -\frac{1}{4}$ in the 1D model (5) for $N = 4$ and $N = 8$ sites, see Fig. 3. In fact, the Hamiltonian (5) is then a product of singlet projection operators in spin and orbital space, so the FM-FO state has the lowest possible energy $E_0 = 0$ and is degenerate with several other states (Fig. 2).

As expected, $C_{ij} = 0$ for $p < -\frac{1}{4}$, and the spin and orbital degrees of freedom disentangle. The situation is qualitatively different above the quantum transition at $p = \frac{1}{4}$, where $C_{ij} \simeq -0.25$ ($C_{ij} = -0.2595, -0.25$ for an $N = 8, 4$ site chain at $p = -0.249$, respectively). Although we are not interested here in accurate quantitative values of the respective intersite correlations, we observe that the $N = 8$ site chain comes already quite close to the thermodynamic limit at the SU(4) point — we found $S_{ij} = T_{ij} = -0.223$ in place of -0.215 for a chain of $N = 100$ sites (which almost reproduces the Bethe ansatz result for an infinite chain) [12]. Furthermore, in the case of $N = 8$ site chain, the data show a smooth decrease of $S_{ij} = T_{ij}$ correlations with increasing p , indicating the tendency towards AF-AO spin-orbital correlations in the regime of large p . This is markedly different from the $N = 4$ site chain, where these correlations are constant ($S_{ij} = T_{ij} = -0.25$) in the entire range of $-\frac{1}{4} < p < \frac{3}{4}$, i.e., up to the SOVB point, where the data suggest a second quantum phase transition to the AF-AO state (Fig. 3a). In fact, this transition is a finite size effect and is replaced by a *smooth crossover* towards smaller values of both S_{ij} and T_{ij} correlations in an $N = 8$ site chain (Fig. 3b).

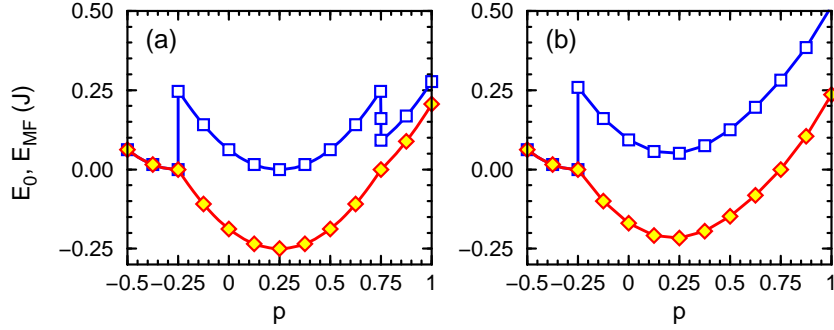


Fig. 4 Ground state energy E_0 (diamonds), and mean field energy E_{MF} (squares) per bond, as obtained for the 1D spin-orbital chains for increasing p in Eq. (5), with: (a) $N = 4$, and (b) $N = 8$ sites.

It is quite remarkable that the composite spin-orbital correlation function (3) has a shallow minimum $C_{ij} = -0.2812$ for an $N = 8$ site chain at the SOVB point, in spite of decreased individual spin and orbital correlations $S_{ij} = T_{ij} = -0.3749$, suggesting rather independent spin and orbital dynamics. Therefore, precisely at this point the entanglement in the exact wave functions $|\Phi_{\pm}\rangle$ shown in Fig. 1 is larger than at the SU(4) symmetric point, where $C_{ij} = -0.2667$. We emphasize that sufficiently long chain with $N = 8$ sites was necessary to reach this conclusion, while shorter chains give inconclusive results, either due to particular stability of the SU(4) singlet for $N = 4$ sites, or due to frustrated four-site singlet correlations for $N = 6$ sites which result in reduced values of $|C_{ij}|$ and E_{MF} (Table I).

In the entire regime of singlet states ($\mathcal{S} = \mathcal{T} = 0$) in the 1D spin-orbital model Eq. (5), one finds large corrections to the mean field energy normalized per one bond,

$$E_{\text{MF}} = \left(\langle \vec{S}_i \cdot \vec{S}_{i+1} \rangle + p \right) \left(\langle \vec{T}_i \cdot \vec{T}_{i+1} \rangle + p \right), \quad (6)$$

as shown in Fig. 4. This demonstrates that one should not decouple spin and orbital operators from each other as this procedure suppresses an essential part of joint spin-orbital quantum fluctuations and leads to inconclusive results. For the same reason, effective magnetic exchange constants obtained by averaging over orbital operators do not represent a useful concept and cannot be introduced in the entangled regime, similar to the realistic spin-orbital models for transition metal oxides [6, 7].

We have verified that quantum entanglement is significant in the SOVB wave functions (Fig. 1) also at higher values of spin S in Eq. (5). However, when spins increase, the AF correlations weaken and AO correlations are enhanced. This may be seen as partial decoupling of slow and fast quantum fluctuations associated with large (small) spin (pseudospin) value, respectively. Indeed, the values of $|C_{ij}|$ and of E_{MF} decrease with increasing S , as shown in Table I.

Table 1 Intersite spin correlations S_{ij} , orbital correlations T_{ij} (2), and composite spin-orbital correlations C_{ij} (3), as well as mean field E_{MF} energy per site (6), obtained for various SOVB phases: for $S = 1/2$ with increasing cluster size of $N = 4, 6$ and 8 sites, and for $S = 1$ and $S = 3/2$ with clusters of $N = 4$ sites. By construction, the exact ground state energy is $E_0 = 0$ in all cases.

S	N	S_{ij}	T_{ij}	C_{ij}	$E_{\text{MF}} (J)$
1/2	4	-0.3500	-0.3500	-0.1600	0.1600
	6	-0.3735	-0.3735	-0.1417	0.1417
	8	-0.3749	-0.3749	-0.2812	0.2812
1	4	-0.2429	-0.3643	-0.0992	0.0992
3/2	4	-0.2050	-0.3690	-0.0806	0.0806

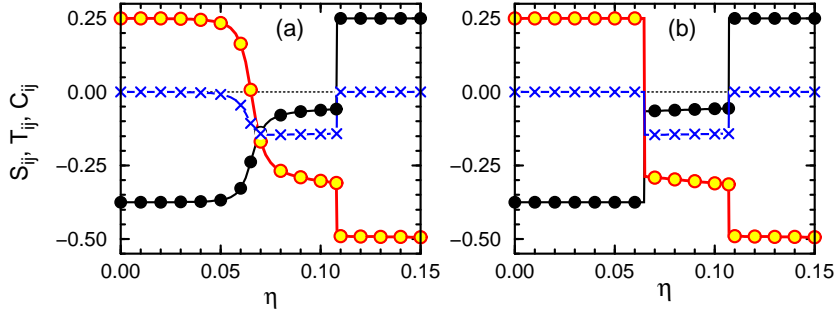


Fig. 5 Intersite spin S_{ij} (filled circles), orbital T_{ij} (empty circles), and composite spin-orbital C_{ij} (crosses) correlations, as obtained with an $N = 4$ site chain for increasing Hund's exchange η in: (a) the vanadate model (1) of Ref. [14], and for (b) the same model without orbital fluctuating terms in Eq. (1). Orbital interactions resulting from GdFeO₃-type distortions are given by $\mathcal{H}_{\text{orb}} = -V \sum_i T_i^z T_{i+1}^z$ with $V = J$, and favor FO order at small η .

Finally, we would like to emphasize that the quantum entanglement is also a common feature of spin-orbital models (1) derived for transition metal oxides when the parameter $\eta = J_H/U$ is small [4]. (Note that large η plays here a similar role to small p in the $SU(2) \otimes SU(2)$ spin-orbital model.) Also in such cases mean field procedure fails and joint spin-orbital fluctuations C_{ij} dominate in the ground state. Such models exhibit even richer behavior than the idealized $SU(2) \otimes SU(2)$ spin-orbital model considered above. In fact, the $SU(2)$ symmetry concerns only spin interactions while it is removed in the orbital sector due to the analytic structure of Coulomb interactions and the multiplet structure of excited states at $\eta > 0$. As a result, one may find *continuous orbital transitions* of the crossover type even when the orbital quantum number \mathcal{T} changes, as shown in Fig. 5a for the vanadate model of Ref. [14] with $S = 1$ spins. However, when the respective interactions are simplified to classical Ising terms (Fig. 5b), such transitions appear to be first order [16], and are qualitatively similar to those encountered usually in the spin sector.

Summarizing, we have demonstrated large quantum entanglement in the $SU(2) \otimes SU(2)$ spin-orbital model for $S = T = 1/2$, which appears to be somewhat stronger in the exact spin-orbital valence bond states of Fig. 1 than at the $SU(4)$ symmetric point. While the spin-orbital entanglement occurs in a discontinuous way in quantum spin transitions, it may appear gradually in continuous quantum transitions which involve orbital degrees of freedom.

Acknowledgements This work was supported by the Polish Ministry of Science and Education Project No. 1 P03B 068 26.

References

- [1] J. B. Goodenough, *Magnetism and the Chemical Bond* (Interscience, New York, 1963).
- [2] L. F. Feiner, A. M. Oleś, and J. Zaanen, *Phys. Rev. Lett.* **78**, 2799 (1997).
- [3] G. Khaliullin and S. Maekawa, *Phys. Rev. Lett.* **85**, 3950 (2000).
- [4] A. M. Oleś, P. Horsch, L. F. Feiner, and G. Khaliullin, *Phys. Rev. Lett.* **96**, 147205 (2006).
- [5] Y. Chen, P. Zanardi, Z. D. Wang, and F. C. Zhang, *New J. Phys.* **8**, 97 (2006).
- [6] G. Khaliullin, *Prog. Theor. Phys. Suppl.* **160**, 155 (2005).
- [7] A. M. Oleś, G. Khaliullin, P. Horsch, and L. F. Feiner, *Phys. Rev. B* **72**, 214431 (2005).
- [8] C. Itoi, S. Qin, and I. Affleck, *Phys. Rev. B* **61**, 6747 (2000).
- [9] S. Miyashita and N. Kawakami, *J. Phys. Soc. Jpn.* **74**, 758 (2005).
- [10] C. K. Majumdar and D. K. Ghosh, *J. Math. Phys.* **10**, 1388 (1969).
- [11] A. K. Kolezhuk and H.-J. Mikeska, *Phys. Rev. Lett.* **80**, 2709 (1998).
- [12] B. Frischmuth, F. Mila, and M. Troyer, *Phys. Rev. Lett.* **82**, 835 (1999).
- [13] Y. Chen, Z. D. Wang, Y. Q. Li, and F. C. Zhang, cond-mat/0606194, unpublished.
- [14] P. Horsch, G. Khaliullin, and A. M. Oleś, *Phys. Rev. Lett.* **91**, 257203 (2003).
- [15] C. Ulrich, G. Khaliullin, J. Sirker, M. Reehuis, M. Ohl, S. Miyasaka, Y. Tokura, and B. Keimer, *Phys. Rev. Lett.* **91**, 257202 (2003).
- [16] S. Miyashita, A. Kawaguchi, N. Kawakami, and G. Khaliullin, *Phys. Rev. B* **69**, 104425 (2004).